Computational Neuroscience - A biological and Mathematical Study of a Neuron

Elizabeth Andreas[1]
Advisors: Prof. Julie Eaton[1] and Lect. Rita (Duong) Than[1]
[1]University of Washington - Tacoma

2019
February

Abstract

Explored in this paper are the biological foundations of singular neuron structure and some mathematical models used to describe their function. After developing understanding of a general neurons biology, the mathematical structure of the resting potential of a neuron given by the Nernst-Plank equation and the Goldman-Hodgkin-Katz equation. Afterward, the Hodgkin-Huxley model is covered in depth and a reduction of the model is used to analyze topological behaviors of neurons. Then an application of studies aimed at the creation of chip implants in damaged parts of the brain, called Brain-Computer Interfaces (BCIs) is briefly introduced.

Contents

1 Introduction

Computational neuroscience is a branch of neuroscience that uses mathematical models to theoretically study the brain, which includes topics such as the development, structure, and even cognitive abilities of the central nervous system (CNS). Explored in this paper are the biological foundations of a single neuron and some mathematical models used to describe their function. After developing an understanding of a general neurons biology, the mathematical structure of the resting potential of a neuron is derived using the Nernst-Plank equation and the Goldman-Hodgkin-Katz equation. Afterwards, the Hodgkin-Huxley model is covered in depth. The Hodgkin-Huxley equations are used to model neural spiking for a single neuron. However, this model is a system of four differential equations and are therefore difficult to solve explicitly. Thus, a reduction of the Hodgkin-Huxley model down to two dimensions is made. The reduced Hodgkin-Huxley model is analysed using phase plane analysis to give a deeper understanding of the topological behaviors of neurons. Given humans have 100 billion neurons, the study of a single neuron may seam trivial. However, the understanding of brain signalling is being applied to many areas of research and development. Which include neurodegenerative disorders that affect this process by slowing down neuron firing. These disorders can inhibit a persons ability to speak or swallow, cause cognitive impairment, difficulty walking and even cause people to go blind. Even in the beginning stages of these conditions, the small changes in the brain can be noticed throughout the body. Research is currently being done in an attempt to correct damage done by neurodegenerative disorders. Of which include studies that are aimed at the creation of chip implants in damaged parts of the brain, called Brain-Computer Interfaces (BCIs).

2 Important Biology for understanding Neural Function

2.1 Neuron Anatomy

In order to understand computational neuroscience, it is important to understand the biology behind the computations. This will give a clear understanding for why certain steps, assumptions and conclusions have been made. Thus, this section breaks down how a general neuron works and where in the body neurons are located. Though knowing the location of neurons is not important for understanding how they work, it does show how a damaged neuron could affect the entire body.

A neuron is a cell in the *central nervous system* (CNS) that sends signals called *action potentials*. There are many different kinds of neurons, however, they all have the same basic structure which can be seen in Figure 1. The *soma* is the body of the cell from which small cable like structures called *dendrites* and axons branch from. Dendrites receives input from other neurons and sends it to the soma and *axons* carry action potentials from the soma to a post-synaptic cell. A *post-synaptic cell* is a term used for a cell receiving information from an axon, it can be a dendrite, a gland, a muscle or even a blood vessel. However, it is by far the most common for an axon to send information to another neuron (via dendrites). Some axons are covered in an insulator called a *myelin sheath* which speeds up the transition of action potentials from one neuron to the next. The connection point between an axon and a target cell is called a *synapses*, most of these cells do not actually touch each other but communicate by the axon sending chemicals (*neurotransmitters*) to the post-synaptic cell. [2]

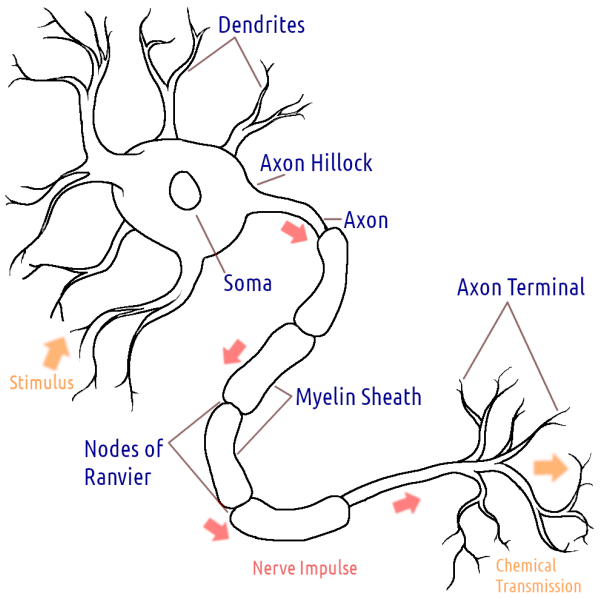

Figure 1: There are many different types of neurons, this image is depicting the general structure and anatomy [1]. All diagrams were drawn by the author. Any source that was consulted in the creation of the image is cited in the caption.

Neurons are made of a *membrane* (lipid bi-layer) which has many types of protein structures embedded into it. *Ion channels* are made up of some of these proteins, which allow for the flow of specific ions in and out of the neuron. The most common and most related to action potentials are sodium ions Na^+, potassium ions K^+, calcium ions Ca^2+ and chlorine ions Cl^-. An electrical potential is created by a difference in the negativity inside the cell verses the outside the cell, this is called *trans-membrane voltage*. When there is no signal being transmitted through the neuron, it settles into a *resting potential*, where this voltage actually settles is different between types of neurons but the most common is around -70 mV.

When a neuron is sending a signal (action potential) the voltage inside the membrane can increase an upwards of 100 mV. *Hyper-polarization* happens when ion channels let positive ions flow out of the neuron or negative ions flow into the neuron. This happens when the neuron is already at its resting state and makes it harder for the cell to fire by inhibiting it. To excite the neuron, it must be made more positive inside the membrane, called *depolarization*. If the neuron is depolarized enough to exceed some threshold then it will cause an action potential to fire through the axon. Immediately after a neuron fires, its negativity will dip below the resting potential and be in an *absolute refractory period* for a short time. At this point it is impossible for the neuron to fire again. This is followed by a *refractory period* where it is very difficult to fire but not impossible. Any signals that a neuron receives that does not lead to an action potential are called *sub-threshold potentials*, however if enough of these signals are sent at roughly the same time they can trigger an action potential. [2]

2.2 Ionic Flow During Electronic and Action Potentials

The voltage changes seen when recording an action potential are the result of ionic flow in and out of the cell membrane. Throughout the rest of this paper, only sodium and potassium ions will be discussed because they play the leading role in action potentials. When a neuron receives a signal from another neuron, a flow of sodium ions cross the membrane into the neuron and increase the voltage inside the membrane, this is called *depolarization*. The positive sodium ions coming into the membrane repel the positive potassium ions already in the neuron, this causes a current to go down the membrane and is called *electrotonic potential spread*. If this was being read by an electrometer, it would show a small spike in the voltage of the cell, however, this is a passive reaction and it soon dissipates as the ions spread through the neuron.

When enough signals come in that causes the inside of the cell to reach a threshold (typically -50 mV), it will trigger nearby voltage gated sodium channels and a flood of sodium will rush in. This causes a significant spike in voltage inside the membrane, which makes inside the membrane more positive than the outside. At around +40 mV, an inactivation mechanism is triggered and stops the flow of sodium ions into the membrane. At this time, voltage gated potassium channels open and potassium ions flow out of the membrane, which causes the cell to drop back down in voltage. Voltage gated potassium channels are not triggered to close until -80 mV. Leaky gates then assist in letting the membrane get back into a resting state at -70 mV by allowing potassium to leak back in (see Figure 2). The sodium channels open and close more quickly than potassium channels, thus having a fast-slow system effect.

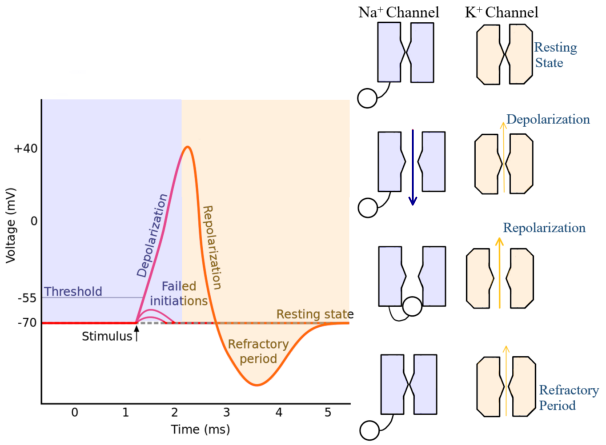

Figure 2: Depiction of ionic flow and voltage gates for the sodium (Na^+) and potassium (K^+) ion channels during an action potential [1].

2.3 The Central Nervous System

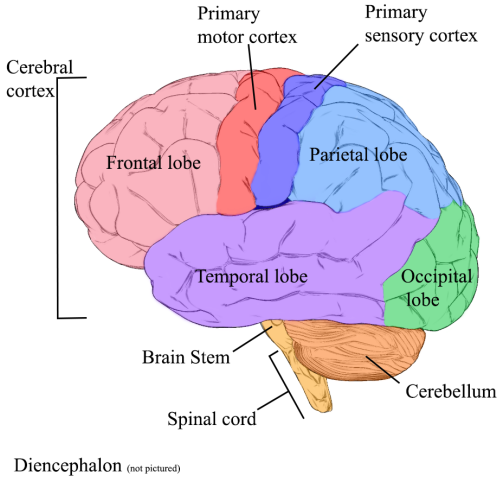

Figure 3: The human brain with a rough layout of the different areas of the CNS [1].

Neurons and fatty tissue make up the entirely of the central nervous system seen in Figure 3 and is vital to all human functions. The spinal cord is apart of the CNS and is composed of neurons. These neurons are the bridge from the brain stem to the rest of the body where signals can be sent to and from nerves, muscles and other functions. This allows the brain to receive sensory information and control movement. The medulla oblongata, the pons and the midbrain all make up the brain stem. This is the communicator between the brain and the spinal cord. The cerebellum controls movement. The thalamus sends sensory inputs to the cerebral cortex and the hypothalamus regulates automatic functions and hormones. The cerebral hemispheres contains the cerebral cortex, basal ganglia, hippocampus and amygdaloid nuclei (amygdala). The basal ganglia regulates moving and is involved in cognitive functions. The hippocampus controls the creation of long term memory and the amygdala plays a hand at the body responses to emotions. The cerebral cortex is made up of four major lobes; frontal, occipital, temporal and parietal. Everything the human body does is a direct result of neural functioning. If something goes wrong in one part of the system, it can affect the entire body. However, if there is no understanding of how a neuron functions then it would be impossible to detect when something goes wrong.

3 Experimental Methods

Resting potential and action potentials can be recorded in two ways, intracellular methods (electrodes enter the membrane of the neuron and can detect sub-threshold fluctuations as well as action potentials) and extracellular methods (does not damage the neural membrane but picks up noise from the surrounding cells). Tracing action potentials between neurons can also be done by specific viruses, dyes or radioactive isotopes of amino acids. Imaging such as fMRIs can show the blood flow of the brain changing when it is performing particular tasks which helps to understand what parts of the brain contribute to certain functions. Electroencephalograms (EEGs) can measure brain activity by placing multiple electrodes across the scalp, but this cannot localize where the signals are coming from [2]. All experimental methods of studying neurons are lacking in some way, they give a clear but very local picture using invasive methods, or they give a wide noisy picture using non-invasive methods. Mathematical models can be used to fill this gap. Using data from experimental methods, models have been created to recreate the signals sent and received by neurons. The most important model to be introduced into neuroscience in the last 60 years is Hodgkin and Huxley's modeling of a signal cell action potential, this model will be introduced later in this paper.

3.1 Resting Potential

To study how a neuron sends a signal, there should be an understanding of the starting point. This would be simple if all of them had the same resting potential, however, they do not. The Nernst equation is used to find these resting potentials using ionic concentrations rather than needing to record it experimentally.

All cells have an electrical voltage (potential difference) between the intra- and extracellular fluids. Due to the lipid membrane separating the fluids, this is often referred to as the *membrane potential* (V_m), measured in millivolts (mV) such that

$$V_m = V_I - V_E, \tag{1}$$

where V_I is the potential on the inside of the cell and V_E is the potential on the outside of the cell. Non-voltage gated ion channels are primarily responsible for establishing resting potential because they allow for a passive flow of ions across the cell membrane. A cell is at its *resting potential* (equilibrium) when the potential across the cell membrane is at rest. Potential differences are due to the differences in concentration of ions on the inside and outside of the cell membrane.

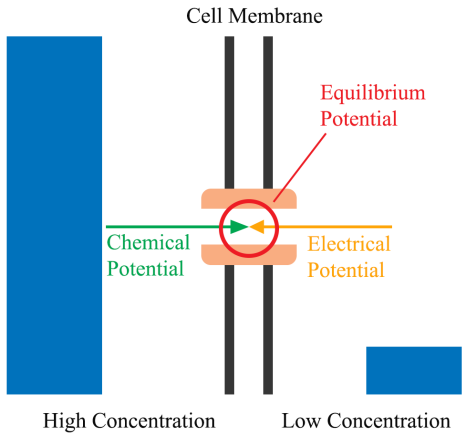

Figure 4: Equilibrium Potential is when the chemical potential and electrical potential between the inside and outside of the cell membrane is equal and opposite [1].

Due to this concentration difference, ions move along their concentration gradient through the channels in the cell membrane (Figure 4). *Chemical potential* quantifies the size of the concentration gradient. Potassium ions are 10 times more concentrated on the inside of the cell verses the outside, so the gradient moves potassium ions out of the cell (called outward current) through non-voltage gated ion channels. This outward current of potassium ions builds up an excess positive charge on the outside of the cell and a buildup of excess negative charge on the inside of the cell. This charge is called the *electrical potential* and inhibits the outward flow of potassium ions. This eventually leads to the cell reaching its resting potential, where the electrical and chemical forces are equal and opposite thus stopping the net flow of ions across the cell membrane which is depicted in Figure 4. The Nernst Equation is a mathematical model used to determine the resting potential and the Nernst-Planck Equation is used to derive the Nernst Equation [3].

3.2 Nernst-Planck Equation

Two main physical forces are responsible for the passive movement of ions across the cell membrane, diffusion (J_{diff}) and electrical drift (J_{drift}). Diffusion can best be described using Fick's Law, which says

that movement across the cell membrane due to diffusion (moles) is proportional to the concentration gradient, such that

$$J_{\text{diff}} = -D\frac{d[C]}{dx} \tag{2}$$

where $[C](x)$ is the concentration of some ion and D is the diffusion constant (mol/cm^3). D is dependent on the size of the ions and the medium it is in (for Na^+ and K^+ the diffusion constant is typically $2.5 \times 10^{-6} cm^2/s$). A version of Ohm's law can be used to describe the electrical drift,

$$J_{\text{drift}} = -\mu z[C]\frac{dV_m}{dx} \tag{3}$$

where $V(x)$ is the membrane potential at some point, μ is a parameter for the mobility of ions (cm^2/Vs) and z is the valence electron number of the ion (for potassium and sodium this would be +1). When the diffusion and electrical drift are added together they give the total flux (J_{total}) across the membrane,

$$J_{\text{total}} = -D\frac{d[C]}{dx} - \mu z[C]\frac{dV_m}{dx}. \tag{4}$$

Given that current can be expressed as $I = J_{\text{total}} zF$, then

$$I = J_{\text{total}} zF = -zFD\frac{d[C]}{dx} - \mu z^2 F[C]\frac{dV_m}{dx}. \tag{5}$$

Using Einstein's diffusion/mobility relation ($D = \frac{KT}{q}\mu$), it is possible to transform the current units of measurement into a more useful format $D = \frac{KT}{q}\mu = \frac{\frac{J}{K}\cdot K}{coulombs}\mu$. If D is then divided by Avogadro's number (mol^{-1}) and substituted into Equation 5, then the final derived version of the Nernst-Plank Equation can be written as,

$$I = -\left(\mu zRT\frac{d[C]}{dx} + \mu z^2 F[C]\frac{dV_m}{dx}\right).$$

When the Nernst-Plank Equation is equal to zero ($I = 0$), it shows that the diffusion and electrical drift are at equilibrium. With differentiation it can be found that

$$V_m = -\frac{RT}{zF}\ln|[C]|.$$

Recall from Equation 1 that $V_m = V_I - V_E$ and note that $[C] = [C]_I - [C]_E$, thus

$$V_m = V_I - V_E = -\frac{RT}{zF}\ln\frac{|[C]_I|}{|[C]_E|}. \tag{6}$$

When derived in this way, the final equation can be used to find the equilibrium potential for each ion and is known as the Nernst Equation [3].

3.3 Goldman-Hodgkin-Katz Equation

The Nernst-Planck equation describes the movement of ions in an aqueous solution (the intra and extracellular fluid). However, the movement of ions across the membrane is more complicated and may not obey this equation. This is because cell membranes have thickness, potential energy barriers and a chance of blocking sites within channels. Thus, passive movement of ions across the cell membrane can be better assessed using a more complex equation, called the Goldman-Hodgkin-Katz (GHK) equation. Although this equation can get complicated quite quickly, the simplified version is what will be discussed here.

The *electrical field* is the gradient of the membrane potential, and is defined as $E = \frac{-dV}{dx}$. If the electrical field is constant, then $E = \frac{-V_m}{L}$ where L is the width of the cell membrane. From the Nernst-Planck equation, μ is used to denote the mobility of the ions.

The GHK equation, which was originally coined the constant-field equation, has three assumptions. The electrical field across the membrane is at a constant state, the Nernst-Plank equation holds true for the intracellular fluid, and the ions move independently from each other. Using these assumptions we can conclude the following,

$$I = -\left(\mu^* zRT\beta \frac{d[C]}{dx} + \mu^* z^2 F\beta[C]\frac{V_m}{L}\right), \quad 0 < x < L \tag{7}$$

where $[C](0) = [C]_I$ and $[C](L) = [C]_E$. The mobility of ions on the inside of the cell is different than the ions on the outside of the cell, thus this is denoted as μ^*. Additionally, β is the ratio of the concentration on the inside of the cell verse the outside of the cell. For example, if $[C]$ is the concentration of the extracellular fluid, the $\beta[C]$ is the intracellular concentration. If we take the integral from 0 to L, we get:

$$I = \frac{\mu^* z^2 F\beta V_m}{L}\left(\frac{-[C]_L + [C]_0 e^{\epsilon}}{(1-e^{\epsilon})}\right), \ \varepsilon = \frac{-zFV_m}{RT} \tag{8}$$

This is often written in terms of permeability, which is defined as $P = \frac{\beta\mu^* RT}{LF}$. This can now be used to rewrite the constant-field equation,

$$I = \frac{Pz^2 V_m F}{RT}\left(\frac{[C]_L e^{\varepsilon} - [C]^0}{e^{\varepsilon} - 1}\right).$$

The constant-field equation tells us the current of a specific ion, however, the resting potential of a neuron is the sum of these individual currents. Assuming that the neurons resting potential is only affected by potassium and sodium ions, then the total current in a resting state is $I = I_K + I_{Na} = 0$. Thus, the resting potential of a neuron can be calculated by

$$I = \frac{P_K z^2 V_m F}{RT}\left(\frac{[K^+]_L e^{\varepsilon} - [K^+]_0}{e^{\varepsilon} - 1}\right) + \frac{P_{Na} z^2 V_m F}{RT}\left(\frac{[Na^+]_L e^{\varepsilon} - [Na^+]_0}{e^{\varepsilon} - 1}\right) = 0$$

which leads to the Goldman-Hodgkin-Katz (GHK) equation,

$$V_m = \frac{RT}{F} ln\left(\frac{P_K[K^+]_L + P_{Na}[Na^+]_L}{P_K[K^+]_0 + P_{Na}[Na^+]_0}\right). \tag{9}$$

4 The Hodgkin-Huxley Model

Beginning in 1938, and again from 1946 to 1952, Alan Hodgkin and Andrew Huxley (Figure 5) studied the electrophysiological behavior of a giant squid axon, which is nearly 100 times larger than our own. Hodgkin found a way to measure the ionic flow of the axon by taking a fine glass tube (diameter $500\mu m$) containing a chlorided silver wire and inserting it through the axon to act as an electrode. This enabled them to record the potential difference between the interior and exterior of the axon, where they discovered what we now know as an action potential. Their work was done at the Physiological Laboratory in Cambridge and at the Laboratory of the Marine Biological Association. Both Hodgkin and Huxley received a Nobel Prize for their work in 1963. [5].

Figure 5: Young Alan Hodgkin (right) and Andrew Huxley (left) during their initial summer of research in 1938. Image sourced from the Marine Biological Association [4].

4.1 Electrical Equivalent Circuits (Conductance Based Models)

Hodgkin and Huxley's model takes the electrical properties of the neuron and explains them using mathematical equations that represent a circuit. This circuit is electrically equivalent to what can be seen during an action potential. Shown in Figure 6, a capacitor represents the *membrane capacitance* (C_m), which is the amount of charge the membrane can store and relates to how fast or slow electrotonic potential spread dissipates. In the original data obtained by Hodgkin and Huxley, the membrane capacitance was between 1.5 $\mu F/cm^2$ and 0.9 $\mu F/cm^2$ but they settled on a constant 1 $\mu F/cm^2$ to simplify the equations. A resistor relates to the sodium (I_{Na}) and potassium (I_K) ion channels that allow flow into and out of the membrane, which includes the leaky gate (I_L) channels. Batteries represent the electrochemical gradient potentials caused by the ion concentrations.

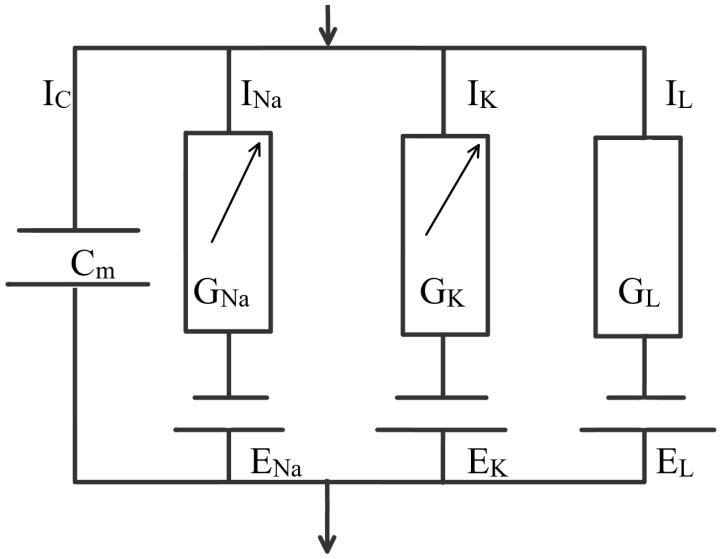

Figure 6: Conductance based model created by Hodgkin and Huxley. C_m is the membrane capacity, G_i is the conductance for the respective ion. E_i is the equilibrium potential for the respective ion. I_c is the total current across the membrane where I_i is the current across each ion channel. Where Na is the sodium channel, K is the potassium channel and L is the leak channel. The arrows are used to signify that I_{Na} and I_K are not constants [1] [5].

The Hodgkin-Huxley model contains two main concepts, he first relates to the membrane capacity (C_m). The charge ($q(t)$) on the membranes surface can be expressed as an instantaneous membrane voltage ($V_m(t)$) and the membrane capacity by the relationship

$$q = C_m V_m. \tag{10}$$

By taking the derivative and realizing that the capacitive current (I_c) is the rate of change of q on the surface of the membrane, then

$$I_c = \frac{dq}{dt} = C_m \frac{dV_m}{dt}. \tag{11}$$

The second major concept adds ionic flux (the flow of ions across the membrane) into the equation. This is known as the total ionic current (I_{ion}) and is the combination of three currents; the sodium current (I_{Na}), the potassium current (I_K) and the leaky gate current (I_L). Kirchoff's first law says that the current across the entire cell membrane must be equal to the flow leaving the cell membrane. Since the total ionic current is either slowed down or sped up by the membrane capacitance, the actual relationship between the internal and external flow of ions can be generalized as

$$C_m \frac{dV_m}{dt} + I_{ion} = I_{ext}, \tag{12}$$

where the externally applied current is expressed as (I_{ext}). This generalized equation gives the overall idea of how the model works but lacks greatly in details because the total ionic flow still needs to be calculated.

Macroscopic ionic current is the flow of I_{Na}, I_K, and I_L through a large number of individual proteins (gates), which make up the ion *channels*, which is related to voltage (V). Ohm's law is used to assume

that the macroscopic ionic current is related to the membrane potential (V_m). Ohm's law is represented by the equation

$$I = \frac{V}{R}$$

which says that the current (I) across a conductor is directly proportional to the voltage (V) across the conductor divided by the resistance (R); in this relationship, resistance is a constant. Ohm's law can then be expressed in terms of conductance such that $G = \frac{1}{R}$, and is more useful in the Hodgkin-Huxley model, so

$$I = GV.$$

In the electrically equivalent circuit (Figure 6), the resting potential (E_i) for each ion channel is represented by the batteries. When taken into account, the current (I) across the membrane is proportional to the conductance (G) across the membrane times the difference in the membrane potential (V_m) and the resting potential, expressed as

$$I = G(V - E). \tag{13}$$

The total ionic current (I_{ion}) can now be expressed as the summation of the macroscopic ionic current across all of the ion channels,

$$I_{ion} = \sum_i I_i = \sum_i G_i(V - E_i) = G_{Na}(V - E_{Na}) + G_K(V - E_K) + G_L(V - E_L). \tag{14}$$

4.2 Gating Variables

Figure 7 shows a cartoon depiction of physical gates, recall that gates are actually proteins embedded in the cell membrane. The gates control the flow of ions through ionic channels, each channel is made up of one or more of these gates. Sodium ions have two types of gates, an activation gate and an inactivation gate. The activation gate allows flow of sodium ions into the cell, in the Hodgkin-Huxley equations the probability of these gates being open or closed is modeled by m. Due to this, these physical gates are usually expressed as the m gate. Though the terminology can be confusing, do not confuse the term "m gate" with the variable m. The h gate is an inactivation gate which prohibits the flow of sodium ions into the cell and is modeled by h. Potassium ions only have one, the n gate that is modeled by n, which allows for the flow of potassium ions out of the cell. Each gate can be *permissive* (open and allowing flow) or *non-permissive* (closed and not allowing flow), when all gates are permissive then the channel is considered *open* and when all of them are non-permissive then the channel is considered *closed*. A voltage gated ion channel type ($i : i = m, n, h$) must be expressed as a probability (p_i) of an individual gate being permissive since any number of gates may be permissive at a given time, this has a range from zero to one. The fraction of gates that are permissive at some time (t) is $p_i(t)$ and $1 - p_i(t)$ is the fraction of gates that are in the non-permissive state at some time (t). The rate at which these gates transition from one state to another is dependent on the membrane voltage and obey first-order rate laws (kinetics).

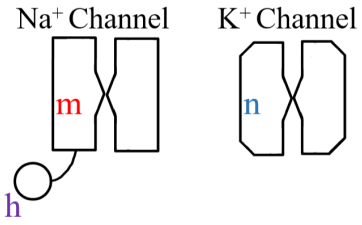

Figure 7: Models of the 3 different protein channels modeled by the Hodgkin Huxley Equations. The sodium channel is modeled by an activation gate (m) and an inactivation gate (h). The potassium channel is modeled by an activation gate (n) [5]. [1]

When transitioning from non-permissive to permissive, the rate variable is annotated by the function $\alpha_i(V)$ and when the gates are transitioning from permissive to non-permissive the rate variable is the function $\beta_i(V)$ and given by the function

$$\frac{dp_i}{dt} = \alpha_i(V)(1 - p_i) - \beta_i(p_i). \tag{15}$$

If the voltage (V) is applied at a constant rate, then the probability of the gates being either permissive or non-permissive will reach a steady state (SS) as time (t) approaches infinity,

$$p_{i\infty} = \frac{\alpha_i(V)}{\alpha_i(V) + \beta_i(V)} \tag{16}$$

and the amount of time that it would take to reach this steady state is expressed with a time constant $(\tau_i(V))$ such that

$$\tau_i(V) = \frac{1}{\alpha_i(V) + \beta_i(V)}. \tag{17}$$

Macroscopic conductance (G_j) with channels type $j : j = Na, K, L$ and gate types $i : i = m, n, h$ is proportional to the product of the individual gate probabilities (p_i) multiplied by a *normalization constant* $(\bar{g}_j)$ which regulates the maximum conductance when all of the gates are permissive, expressed as

$$G_j = \bar{g}_j \prod_i p_i \tag{18}$$

and can be broken down further into the probabilities of different types of gates being in a permissive or none permissive state. Hodgkin and Huxley developed these functions by fitting it to their experimental data and the biological functions of the neuron. Interestingly though, Hodgkin and Huxley could only break down the probabilities of the different gates by fitting the model to the data they had collected. During their experiments, Hodgkin and Huxley were able to separate the potassium current during a spike using a voltage clamp technique. This allowed them to study its ionic flow without the interference of the sodium ionic flow. In doing this, they found that potassium flow had an increase that was similar to a sigmoid function but had a decrease rate similar to that of exponential decay. The mathematical model that was found to best fit this curve was a polynomial function of n^4 (recall this n is the probability of gates being permissive).

The activation m and inactivation h were also modeled in a similar fashion. However, h is the inactivation of m so they must be modeled together. Recall that the gates are modeled numerically as the probability that all the gates will be open or closed within a channel and is a value between zero (all closed) and one (all open). The m activation starts near zero but increases to one quickly, allowing a quick influx of sodium ions into the cell. Since the inactivation of the sodium current is modeled by h, it starts at one and slowly decreases to zero [2]. The polynomial function that best fits these two underlying processes was m^3h. Although they could not find an underlying biological reason, they were able to find that

$$G_{Na} = \bar{g}_{Na} m^3 h \quad \text{and} \quad G_K = \bar{g}_K n^4.$$

Notice that the leak gate isn't written in terms of macroscopic conductance, this is because this gate is perceived as a constant in the Hodgkin-Huxley model. When these are substituted into the equation for the total ionic current (14) then we get the standard notation of the Hodgkin-Huxley equations, which ends up being a system of four differential equations such that

$$C_m \frac{dV}{dt} = I_{ext} - \bar{g}_{Na} m^3 h (V - E_{Na}) - \bar{g}_K n^4 (V - E_K) - g_L (V - E_L), \tag{19}$$

$$\frac{dm}{dt} = \alpha_m(V)(1 - m) - \beta_m(V)(m), \tag{20}$$

$$\frac{dh}{dt} = \alpha_h(V)(1 - h) - \beta_h(V)(h), \tag{21}$$

$$\frac{dn}{dt} = \alpha_n(V)(1 - n) - \beta_n(V)(n). \tag{22}$$

The functions $\alpha_i(V)$ and $\beta_i(V)$ are different for each gate and can vary across different types of neurons. However, Hodgkin and Huxley used the following

$$\alpha_m = 0.1 \frac{25 - V}{e^{\frac{25-V}{10}} - 1}, \quad \beta_m = 4e^{\frac{-V}{18}} \tag{23}$$

$$\alpha_h = 0.07e^{\frac{-V}{20}}, \quad \beta_h = \frac{1}{e^{\frac{30-V}{10}} + 1} \tag{24}$$

$$\alpha_n = 0.01 \frac{10 - V}{e^{\frac{10-V}{10}} - 1}, \quad \beta_n = 0.125e^{\frac{-V}{80}}. \tag{25}$$

5 Analysis Methods Introduction

While there are ways of finding numerical approximations to the Hodgkin-Huxley model (see a few in Appendix A), they do not help in the understanding of how the entire system works together. This has lead to the creation of many analysis methods that help us understand the Hodgkin-Huxley model. Two of these models, the FitzHugh-Nagumo model and the Morris-Lecar model, can be seen in Appendix B and are useful tools to understanding the more complex simplification addressed later, a two-dimensional reduction of the Hodgkin-Huxley equations.

Before the reduction model can be explained it is important to introduce autonomous system phase planes which is needed to fully analyse the model. The van der Pol equations will be used for this introduction, though it will not be used directly in the analysis model, the van der Pol equations are similar in many ways and chosen to deepen the understanding of concepts needed for the two-dimensional reduction of the Hodgkin-Huxley equations.

5.1 Autonomous System Phase Planes

Phase plane analysis is a geometric method used to study two-dimensional autonomous systems on a global scale rather than with time, such that $x' = f(x, y)$ and $y' = g(x, y)$. The solutions are parametric curves plotted by $C(t) = t, x(t), y(t)$. For an autonomous system, the tangent vector $\vec{T}$ to $C(t)$ at any point (x, y) can be found without solving the system and is equal to $x'(t)\vec{i} + y'(t)\vec{j}$.

A *phase plane* is a set of vectors forming a directional field in the xy-plane. This set is obtained by finding the tangent vectors along a grid (x_i, y_i) for the two dimensional system $x' = f(x, y)$ and $y' = g(x, y)$. When a phase plane is created, it is possible to have a geometric representation of how solutions behave given different initial values. When solution curves are drawn onto the phase plane showing how solutions in all parts of plane behave, it is called a *phase portrait*.

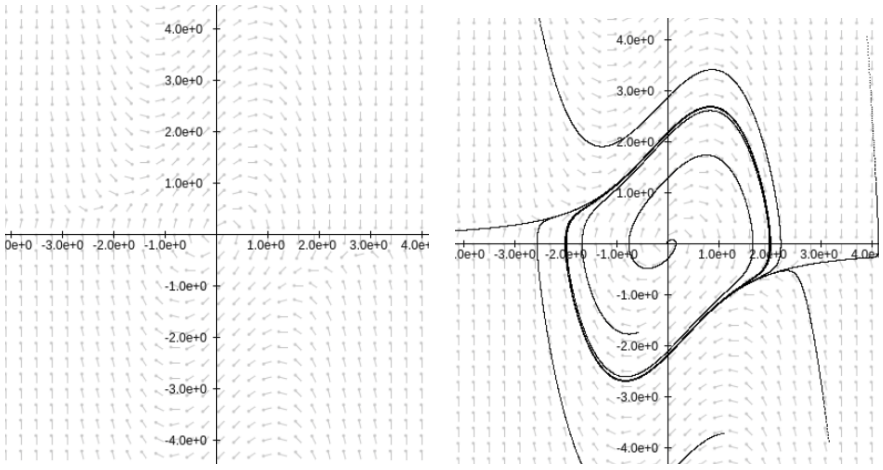

Figure 8: Phase Plane (Left) and Phase Portrait (Right) of the van der Pol equation. [6]

Shown in Figure 8 is the phase plane and phase portrait representing the two dimensional form of the van der Pol equation such that

$$x' = y$$
$$y' = -x + y(1 - x^2).$$

It is possible to see how initial conditions affect this system. When starting near the origin, the system is unstable and the solution curve will begin to oscillate away from zero and enter a *limit cycle* where it continues on to oscillate in a fixed pattern for all time (t). If starting far from the origin the system has a damping affect and pulls the solution curve in towards the limit cycle. This relationship can easily be seen in Figure 9.

An *equilibrium solution* of a two-dimensional system is where the tangent vector $\vec{T} = 0$, meaning both $x' = f(x, y) = 0$ and $y' = g(x, y) = 0$ simultaneously. Once a system is at equilibrium, it will stay there and show up as a single point within the phase plane. However, they represent an entire solution curve

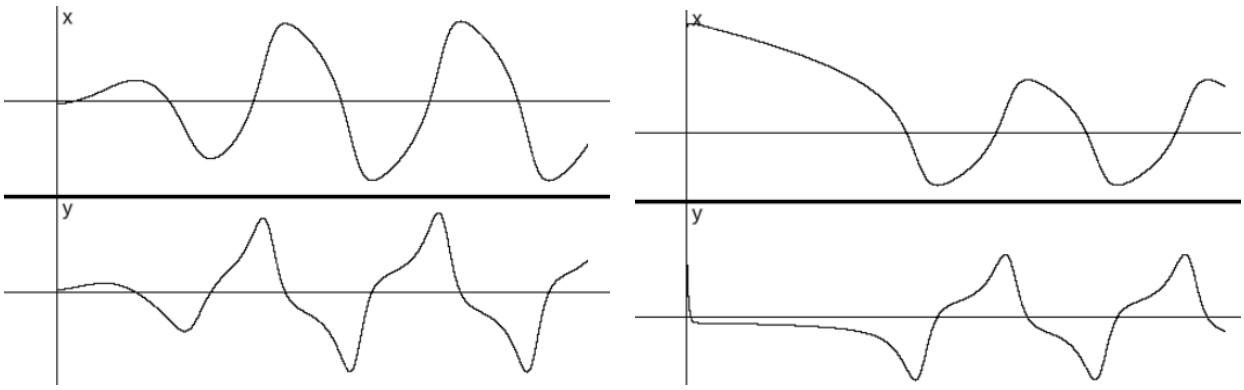

Figure 9: View of $x(t)$ and $y(t)$ graphed separately against time (t) for an initial value close to the center (Left) and far from the center (Right) of the van der Pol equation phase plane. [6]

for $-\infty < t < \infty$. A nonlinear system can have many equilibrium points, of which exact coordinates may not be able to be solved for analytically. In this case, the Hartman-Grobman Theorem can be used to describe the behavior about the equilibrium solutions. However, this theorem requires the use of *nullclines*, a special type of isocline. An isocline is a curve in the plane where it is constant, the null isocline (nullcline) is specifically when that curve is zero.

For example, in a phase plane for the equations $x' = f(x, y)$ and $y' = g(x, y)$ both $x' = 0$ or $y' = 0$ are nullclines for the system. Setting $f(x, y) = 0$ to find a nullcline for x' creates a vertical tangent vector in the phase plane. Similarly, when $g(x, y) = 0$ the tangent vector will be horizontal. If all of the nullclines for x' and y' are sketched onto a phase plane, the points of intersection between the x' and y' nullclines represent the equilibrium solutions for the system. Figure 10 shows the nullclines curves for the van der Pol equations. The x' and y' nullclines intersect at the origin and represent the only equilibrium solution for the entire system of equations, although a system in general can have more than one point of intersection between the nullcline curves.

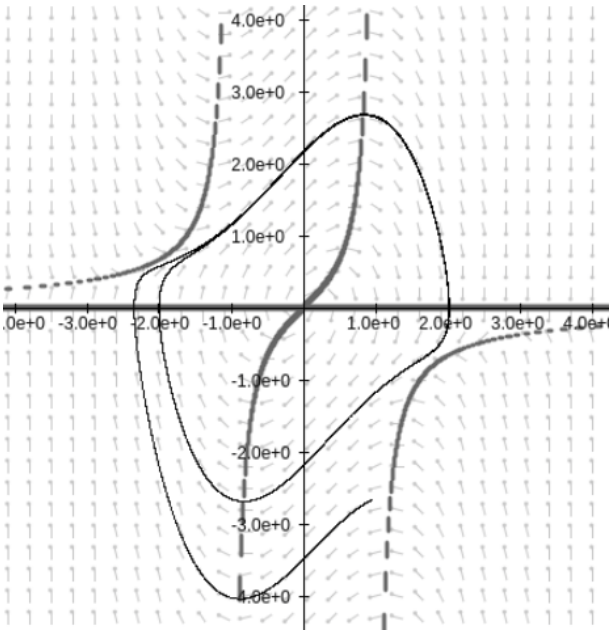

Figure 10: Nullcline curves for the van der Pol equations. The three vertical lines represent the y' nullcline. The x' has a nullcline along the x-axis. [6]

There are different types of equilibrium points and A *Jacobian matrix* J can be used to evaluate them using the trace and determinant of J such that

$$J = \begin{bmatrix} \frac{\partial f}{\partial x} & \frac{\partial f}{\partial y} \\ \frac{\partial g}{\partial x} & \frac{\partial g}{\partial y} \end{bmatrix}, \quad tr(J) = \frac{\partial f}{\partial x} + \frac{\partial g}{\partial y}, \text{ and } \det(J) = \frac{\partial f}{\partial x} \cdot \frac{\partial g}{\partial y} - \frac{\partial g}{\partial x} \cdot \frac{\partial f}{\partial y}.$$

Table 1 is a reference for finding the type of equilibrium at the origin for a linear system. For a system that is non-linear, the Hartman-Grobman Theorem says that in a small region around the equilibrium point, the behavior of a non-linear system has a behavior that is similar to that of a linear system at the origin. Therefore, as long as the trace does not equal zero, the trace and determinant of J can be compared to a linear system using Table 1 to determine what the equilibrium type is. This table was derived using eigenvalues and eigenvectors but that derivation is out of the scope of this paper, reference [7] for more information on this topic.

Table 1: Determining type of equilibrium at the origin for a linear system

Case	Equilibrium Type	$\det(J)$	tr(J)	$tr(J)^2 - 4\det(J)$
1	sink	+	-	+
2	source	+	+	+
3	saddle	-	arbitrary	+
4	center	+	0	-
5	spiral sink	+	-	-
6	spiral source	+	+	-

When solution curves go directly to an equilibrium point it is considered stable and called a sink. Conversely, a source is when all the solution curves lead away from the equilibrium point and is considered unstable. When most solutions lead away from the equilibrium point, but not all, it is called a saddle point. A center is when the solution curves have concentric ellipses around it. When all of the solutions cycle periodically to the equilibrium point it is called a spiral sink and is considered a stable point. Lastly, a spiral source is the opposite of a spiral sink, such that the solutions cycle periodically away from the equilibrium point and is unstable.

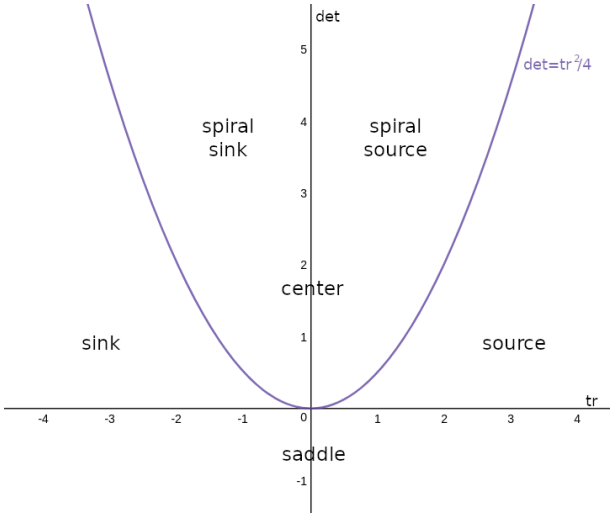

Figure 11: Depiction of the trace-determinate plane showing all of the equilibrium behaviors in Table 1. [1]

These changes in behavior can also be seen by plotting the trace and determinant together in the xy-plane, called a *trace-determinant plane* (Figure 11). Using this is similar to using Table 1, when the determinant and trace are positive and the equilibrium point is above the curve $\det = \mathrm{tr}^2/4$ then the point acts as a spiral source. For two dimensional systems that have a parameter, using the trace-determinant plane can be useful in understanding changes in the behavior of an equilibrium point. To get an understanding of this, a parameter (μ) can be introduced to the van der Pol equation to see how the behavior of the system depends on μ

$$x' = y$$
$$y' = -x + \mu y(1 - x^2).$$

It was already shown that the equilibrium point for the van der Pol equation is at the origin, thus

$$J(0,0) = \begin{bmatrix} 0 & 1 \\ -1 + 2xy\mu & \mu(1-x^2) \end{bmatrix} = \begin{bmatrix} 0 & 1 \\ -1\mu & \mu \end{bmatrix},$$

$$(J) = 0 + \mu = \mu,$$
$$\det(J) = 0 \cdot \mu - (-1) \cdot 1 = 1.$$

Referring to Figure 12 or looking back at table Table 1, when $\mu = 1$ it is easy to see that the equilibrium point is a spiral source which can be visually verified by looking at Figures 8 and 9. However, the system changes from a spiral source at $\mu = 1$ to a spiral sink if $\mu = -1$. What makes the trace-determinant plane so useful in a system with a single parameter is that the parameter can be plotted on the plane, as seen in Figure 12. Since the determinate in this system is always equal to one μ can be plotted along this line. As μ goes from $-\infty$ to ∞, the equilibrium point will change behavior suddenly three times, at both points where it intersects the curve $\det = \mathrm{tr}^2/4$ and when it crosses over the det-axis. In general, when a system has a sudden qualitative change in its equilibrium behavior as the parameter passes some value then this is called a *bifurcation*. For more in-depth information on this topic, refer to Virginia W. Noonburg book on Ordinary Differential Equations [7].

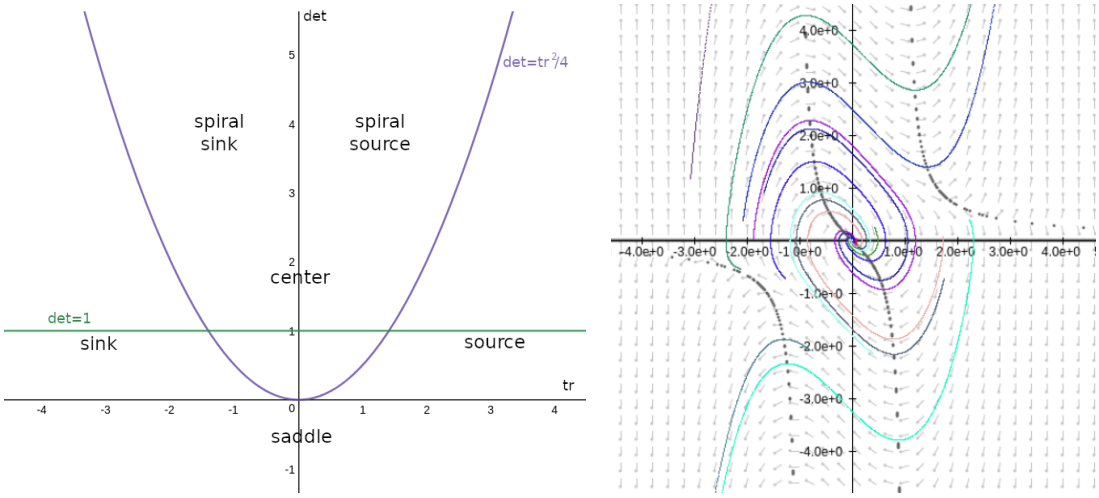

Figure 12: The plot to the left is depicting the range of the parameter μ (green) on the trace-determinate plane. To the right is the phase portrait of the van der Pol equations when $\mu = -1$. [6] [1]

5.2 Bifurcations

There are many different types of bifurcations, however the focus here will be on *local bifurcations*. These occur when a parameter of a system causes the equilibrium point to change behavior, better described as a change in the stability of the equilibrium point. An example of this was shown with the van der Pol equations.

There are different types of local bifurcations , the most notable for the two-dimensional study of the Hodgkin-Huxley model are saddle-node and Hopf bifurcations . When a system has two-fixed points that intersect (collide) with each other then it is called a *saddle-node bifurcation*. A *Hopf bifurcation* is when a system has the sudden onset of a limit cycle. When stable and large amplitude oscillations occur suddenly, it is called a *sub-critical Hopf bifurcation*. This type requires that a spiral sink or sink change into an spiral source or source and is surrounded by a stable limit cycle. When the oscillation amplitude starts off small and increases as the parameter is increased it's called a *super-critical Hopf bifurcation*.

6 Two-dimensional Reduction Model

Though the Hodgkin-Huxley model has been undeniably useful in neuroscience, it is difficult to solve for solutions without the aid of numerical approximations. By taking away some of the complexity of this model, it is possible to study why neurons behave the way they do. The two-dimensional reduction model in particular can show why a neuron might change from a bursting behavior, spiking only to stimulus, to an oscillatory behavior, continuous spiking. To reduce the four-dimensional Hodgkin-Huxley model down to a two-dimensional model requires some assumptions. The first is that the the sodium ion inactivation h can actually be modeled as the a function of n such that

$$h = 0.8 - n. \tag{26}$$

Looking at Figure 13, this inverse relationship can easily be seen since h is essentially a vertical flip of n. The second assumption is that sodium ion activation m can be modeled as a steady state

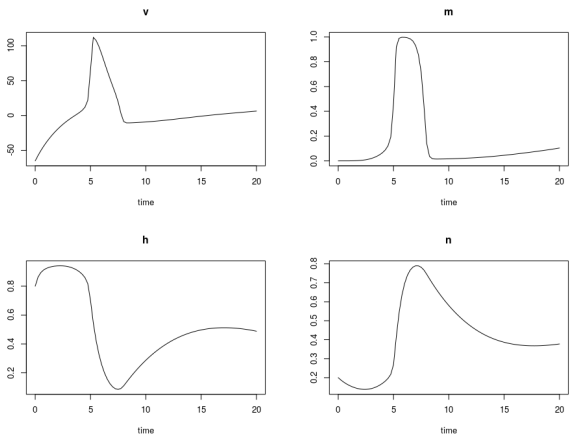

Figure 13: The ion activation and voltage during an action potential, all with time (ms). Top left is voltage, top right is Na^+ activation. The bottom left is Na^+ inactivation and bottom right is K^+ activation. Note how the bottom two graphs are inverse of each other. [8]

function (see equation 16). This assumption is made because the sodium ion flow increases, decreases and reaches a steady state on a much faster time scale than potassium ion flow n.

By making these two assumptions, a system of two equations can be made by using equation 26 to simplify equation 19, which can then be used to compile equation 27. Notice how both equations that model the m and h are no longer needed. This is because h is now being modeled by n and although m still needs the steady state equation to find its value, it is only dependent on voltage and is no longer a probability equation. So the system can now be modeled using

$$C_m \frac{dV_m}{dt} = -\bar{g}_{Na} m_\infty^3 (0.8 - n)(V_m - E_{Na}) - \bar{g}_K n^4 (V_m - E_K) - g_L (V_m - E_L) + I_{ext} \tag{27}$$

$$\frac{dn}{dt} = \alpha_n (1 - n) - \beta_n n \tag{28}$$

where all gating probabilities are modeled using the same values as in equations 22-25. Given the two-dimensional reduction model, it is now possible to analyse by introducing variables into the system. Both the membrane potential (V_m) and the potassium ion gate activation (n) are the variables and what will be analysed. The externally applied current (I_{ext}) will be the parameter used to change how the system behaves. The membrane conductance (C_m) will be set to $1\mu F/cm^2$. The sodium and potassium maximal ion conductance's, $\bar{g}_{Na}$ and $\bar{g}_K$ will be set to 120 $\mu A/cm^2$ and 36 $\mu A/cm^2$ respectively and the leaky gate (g_L) is set at 0.3 $\mu A/cm^2$. The resting potentials of sodium and potassium are 115 $\mu A/cm^2$ and -12 $\mu A/cm^2$. Lastly, the neuron resting potential is set to 10.6 $\mu A/cm^2$. Notice how before it was stated that the resting potential of an general neuron is around -70 mV and the peak of an action potential is around $+40$ mV, the difference between these two values is 110 mV. However, in the analysis of this model, the membrane potential has been adjusted so that the resting state of the neuron is 0 mV and the maximum membrane potential during an action potential is 110 mV. This will still give the same results but makes computation easier. Reference Table 2 to get a summary of all of the parameters and general values that will be used throughout the rest of this section. Though out of the scope of this paper, Christof Koch's book on the Biophysics of Computation explains in detail why these values are used to analysis the reduced model of the Hodgkin-Huxley equations.

Table 2: Summary of parameters in the Hodgkin-Huxley model and introduction of constants to give a generalize model of a neuron.

Parameters	**Values Used to Analyze**
V_m - membrane potential (mV)	Variable
n - potassium activation	Variable
I_{ext} - externally applied current ($\mu A/cm^2$)	Parameter
C_m - membrane conductance ($\mu F/cm^2$)	$C_m = 1$
$\bar{g}_{Na}$ and $\bar{g}_K$ - maximal ion conductance ($\mu A/cm^2$)	$\bar{g}_{Na} = 120$, $\bar{g}_K = 36$
g_L - leak conductance ($\mu A/cm^2$)	$g_L = 0.3$
E_{Na} and E_K - ion resting potentials ($\mu A/cm^2$)	$E_{Na} = 115$, $E_K = -12$
E_L - neuron resting state ($\mu A/cm^2$)	$E_L = 10.6$
$\alpha_n = 0.01(\frac{10-V_m}{exp(\frac{10-V_m}{10})-1})$	$\beta_n = 0.125exp(\frac{-V_m}{80})$
$\alpha_m = 0.1(\frac{25-V_m}{exp(\frac{25-V_m}{10})-1})$, $\beta_m = 4exp(\frac{-V_m}{18})$	$m_\infty = \frac{\alpha_m}{\alpha_m+\beta_m}$

6.1 Phase Plane Analysis

Beginning the phase plane analysis is best done by finding the nullclines. Recall that the nullclines for the van der Pol equations were found by setting the equations in the system equal to zero. Here that is accomplished by setting $\frac{dV_m}{dt} = 0$ and $\frac{dn}{dt} = 0$. When graphed, it results in the nullcline portrait shown in Figure 14 when there is no externally applied current ($I_{ext} = 0$) to the system.

The intersection of the nullclines for $I_{ext} = 0$, is the equilibrium, which is approximately $(-0.1957, 0.3147)$. When the Jacobian matrix is used to analyse this point it can be found the equilibrium behaves as a sink. To verify this behavior, a trajectory of two different initial values, $V_m = 0, n = 0$ and $V_m = 20, n = 0.2$ can be evaluated. It can be seen in Figure 14 that for both initial values, the membrane potential increases

towards 115 mV but the probability of the potassium ion channels being permissive hardly changes at all. At approximately 115 mV, The probability of the potassium ion channels being permissive increases rapidly, allowing flow of potassium ions out of the system which decreases the voltage. At approximately -10 mV, the potassium gates close and the system sinks into the equilibrium point. This is exactly what is seen during an action potential and when the behavior of the phase plane is plotted against time, the characteristic spike is easily recognizable.

Interestingly, increasing the parameter I_{ext} drastically changes the behavior of the equilibrium point. If the external current is increased to 15, the system experiences a Hopf bifurcation and the two initial values no longer sink to the equilibrium point. Instead, the system enters a limit cycle which can be seen in Figure 14. To fully grasp what is happening to the system as the current is increases from $I_{ext} = 0$ to $I_{ext} = 15$, the membrane potential and the potassium activation can be plotted against time, which is also seen in Figure 14. This is representative of a neuron when is changes from an excitable behavior (only spiking to a stimulus) to a bursting behavior (continual spiking).

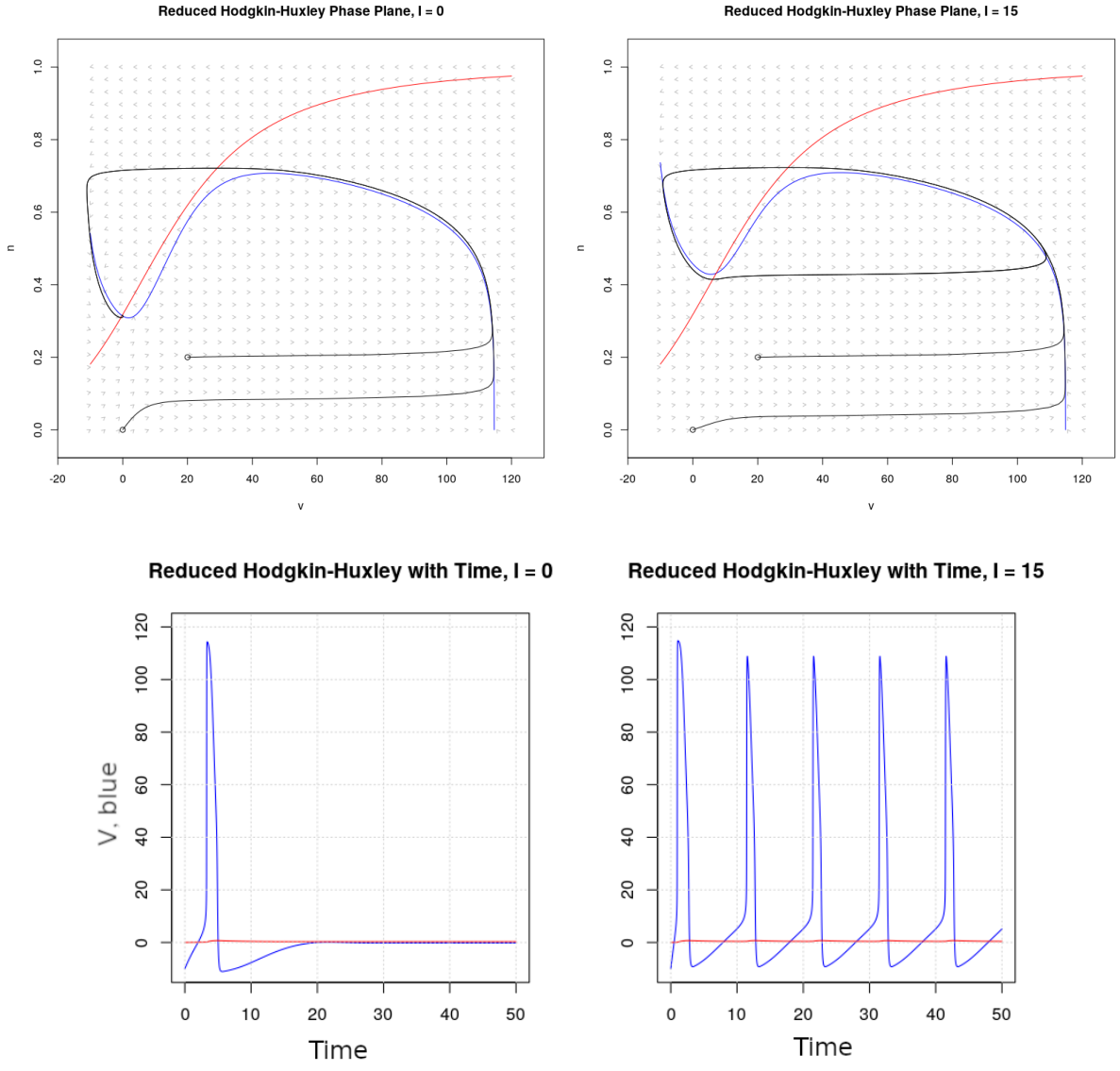

Figure 14: By setting the reduced model equations equal to zero, we get the critical point set called nullclines, shown in the upper two phase planes. The red curve is when $\frac{dn}{dt} = 0$ and the blue curve is when $\frac{dV_m}{dt} = 0$ The intersection of these tell us where our equilibrium solutions are. The graphs on the bottom show how initial values behave in the system over time [**?**]. [8]

So far, this reduced system has shown two different equilibrium point behaviors, a sink and a limit cycle, as the current to the system is increased. However, this model can also can be modified to show different types of behaviors. To accomplish this, the sodium activation h needs to be modeled in a slightly different way, such that

$$h = 1 - n. \tag{29}$$

Figure 15 shows that there are now three intersections in the nullclines when there is no externally applied current. If each of these points were to evaluated using the Jacobian Matrix, it would be found that the lower left point still acts as a sink, the upper point acts as a source and the middle point is a saddle. What is interesting about this adjustment is that when the system bifurcates and enters into a limit cycle at $I_{ext} = 15$, the saddle point and the sink collide with each other. This means that the system is experiencing a saddle-node bifurcation, which can also be seen in Figure 15. Notice that the spike width between the reduced model in Figure 14 is smaller than in the modified reduced model shown in Figure 15. This is happening because it is taking longer for the potassium activation to increase.

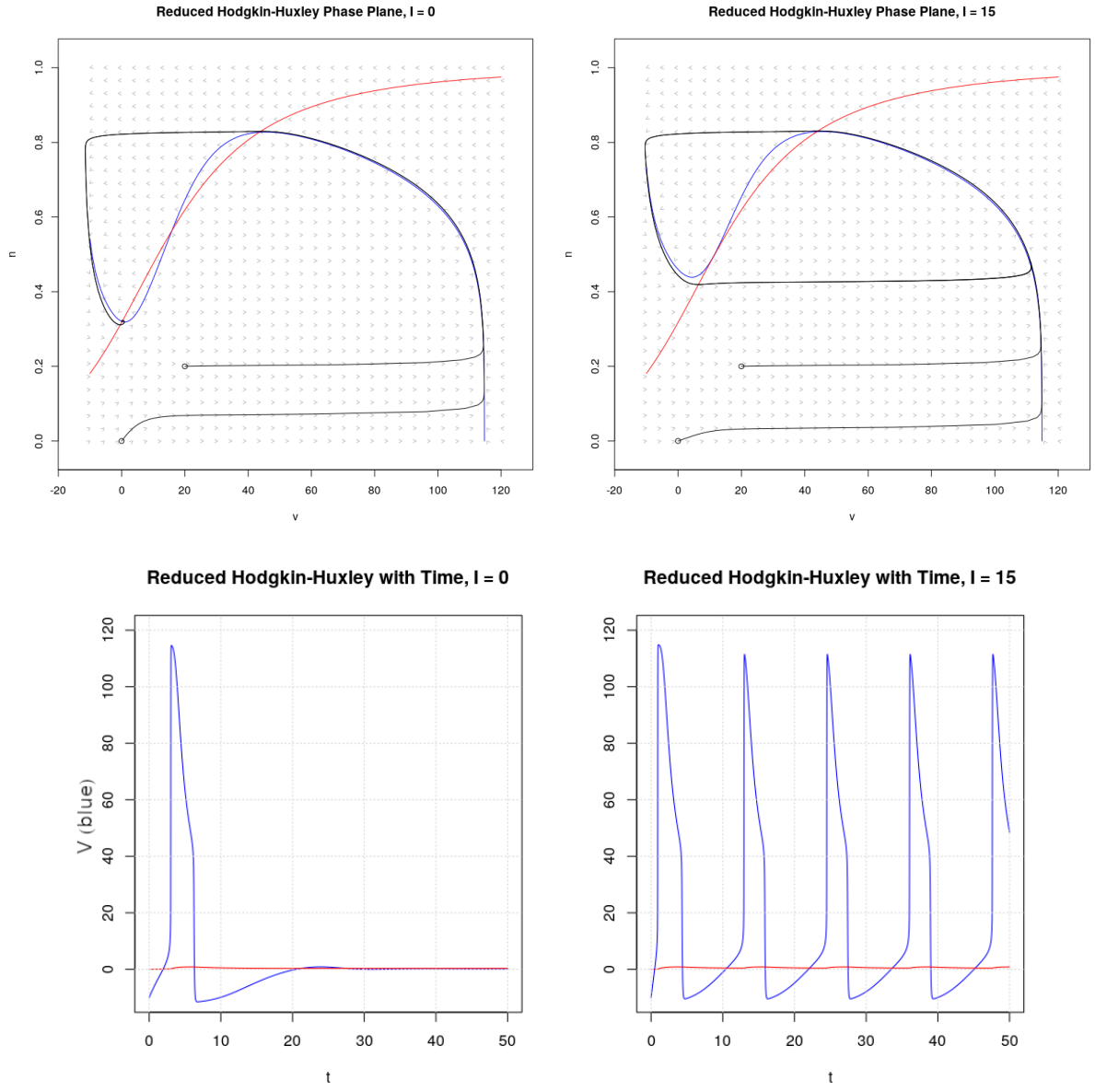

Figure 15: Nullcline solutions for a modified version of the reduced model when $I_{ext} = 0$ (left) and $I_{ext} = 15$ (right). When there is no applied current, the system has three equilibrium points. When the current is increased to 15, a saddle-node bifurcation occurs [5]. [8]

Analysing the reduced model of the Hodgkin-Huxley equations has shown to be a powerful tool in understanding neural phenomena. In particular it has shown why a neuron spikes and why it might change between two modes of operation, excitable or bursting. It has also shown how a simple change to the system might drastically change how it behaves. The advantage to using the reduced model is that it gives qualitative information about these changes without necessarily needing every biophysical detail. Reducing the amount of information needed to study one neuron in turn will reduce the amount of information needed to study a network of neurons as well as reducing the computational load of doing such a task. Although removing details makes it easier to get an overall picture of what a neuron or a system of neurons is doing, it also has a disadvantage in not being able to give quantitative results.

7 Motivation

Even small changes to the Hodgkin-Huxley equations can dramatically affect how the system behaves. Take, for example, the general neuron described using the parameters from Table 2. The four images to the left in Figure 16 show the voltage, as well as m, n, and h gate permissive probabilities during an action potential without any applied current. If the probability of potassium activation is adjusted very slightly, but nothing else in the system is changed, the neuron enters directly into a limit cycle which is seen in the right four images in Figure 16. This is only an example of how one small change in one neuron can affect the stability of the system.

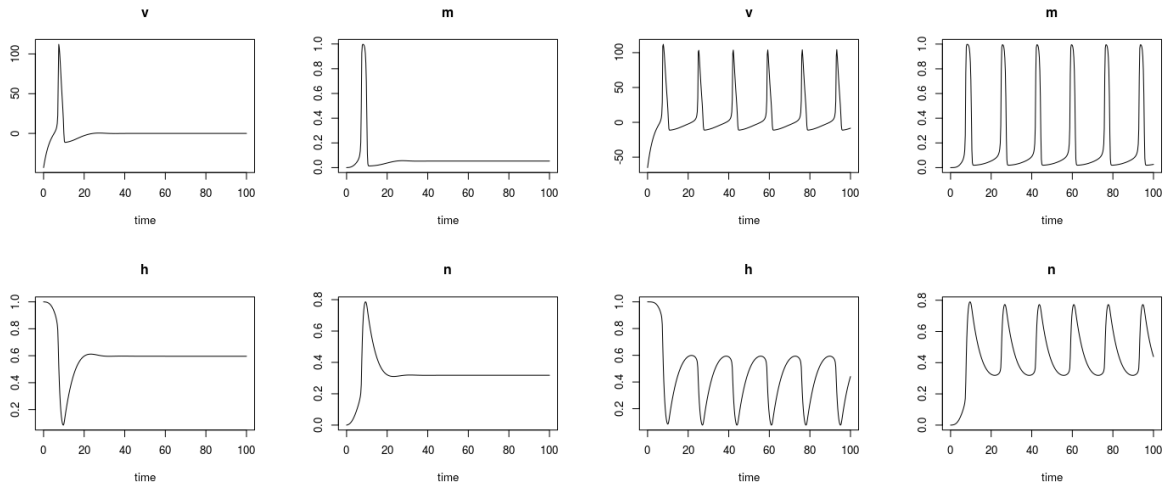

Figure 16: The four graphs to the left show the change in voltage, n, m, and h gate probabilities with time during an action potential. This is in an axon with the same parameters as the ones in Table 2 with no current added to the system. The four photos to the right are showing the same neuron with only the change being a slight adjustment to the probability of the n-gate being in a permissive state. [8]

There are approximately 100 billion neurons and over 100 trillion synapses in the human brain, all working together in a delicate synchronization. Neurodegenerative disorders affect this process by slowing down neuron firing. This can happen in a number of ways, some chronic disorders work by destroying the insulating fat surrounding axons (myelin sheaths), seen in Multiple Sclerosis (MS) and Amyotrophic Lateral Sclerosis (ALS). Others, like Parkinson's disease, inhibit neurotransmitters from being released which affects how neurons communicate with each other. Unfortunately, once neurons are damaged they can't fully repair. The body can remyelinate but the process is slower than many of the conditions that destroy it. These are chronic, progressive disorders that can cause any number of symptoms such as muscle weakness, coordination issues, stiff muscles and muscle spasm. They can inhibit a persons ability to speak or swallow, cause cognitive impairment, difficulty walking and even cause people to go blind. ALS often results in death due to lung issues and the life span of people with MS and Parkinson's is shorter than average. Even in the beginning stages of these conditions, the small changes in the brain can be noticed throughout the body. Understanding how neurons fire and communicate with each other is critical in understanding why neurodegenerative disorders begin and how they affect the body.

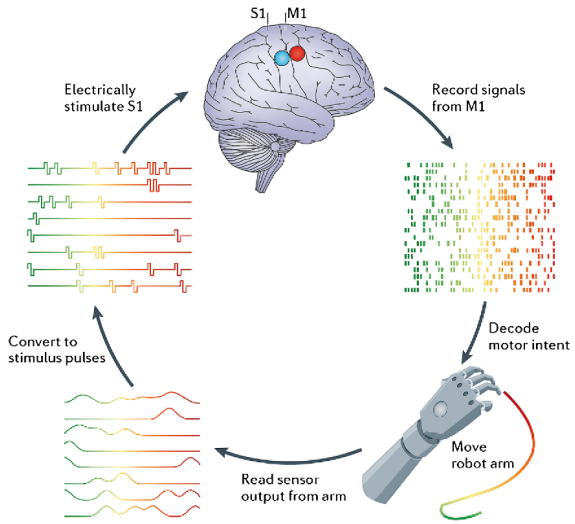

Figure 17: General concept of Brain-computer interfaces (BCIs).

This understanding isn't only important to find the causes of these conditions but also in creating ways to make peoples lives easier when they have already been affected by them. Currently, the understanding of brain signalling is being applied to many areas of research and development to correct these disorders, one of which is the creation of Brain-Computer Interfaces (BCIs). BCI's, placed in damaged areas of the brain, are mechanical devices that analyze brain signals and translate them into commands the the body would normally be able to do on its own. The main goal of BCI's is to replace or restore useful functions in people who are affected by neurodegenerative disorders. Figure 17 gives a general depiction of how these devices work. The development of these devices is being done at many places around the world, including the University of Cambridge and by a company created by Elon Musk called Neuralink.

A Numerical Methods

Though it was already mentioned that the Hodgkin-Huxley model is a system of four differential equations, it is worth mentioning that this system does not have explicit solutions that are comprised of simple functions. However, it is possible to approximate solutions using numerical methods. The simplest of which are outlined in this section.

A.1 Forward Euler's Method

The Euler's method is the simplest method for approximating solutions to ordinary differential equations (ODE's). It uses a combination of tangent lines to make a piecewise linear function that provides an approximation of an actual solution to the ODE. Consider the first order differential equation,

$$\frac{dy}{dt} = f(t, y), \quad y(t_0) = y_0.$$

If $\frac{dy}{dx}$ and f are continuous then there exists a unique solution such that $y = \phi(t)$ on some interval surrounding the initial point [2]. Using the Euler's Method, we can approximate $y = \phi(t)$ by the manipulating the derivative equation $\frac{dy}{dt} \approx \frac{(y_{n+1}-y_n)}{\Delta t} = f(t_n, y_n)$ to produce the difference equation

$$y_{n+1} = y_n + \Delta t f(t_n, y_n)$$

where $y_0 = (t_0)$ and $t_0 = (t + n\Delta t_0)$. This final notation is what is known as the Forward Euler's Method, and is used by calculating each slope and taking a step in that direction such that

$$\begin{aligned}
y_1 &= y_0 + \Delta t f(t_0, y_0) \\
y_2 &= y_1 + \Delta t f(t_1, y_1) \\
y_3 &= y_2 + \Delta t f(t_2, y_2) \\
&\vdots \\
y_n &= y_{n-1} + \Delta t f(t_{n-1}, y_{n-1}) \\
y_{n+1} &= y_n + \Delta t f(t_n, y_n).
\end{aligned}$$

This method is simple because all you have to do is explicit (plug in and calculate) calculations. However, the larger the step size (Δt) used in the approximation of $y = \phi(t)$ the less accurate this method becomes. If the step size is cut in half, the error in the approximation is also reduced by a half. This error denoted as $\mathcal{O}(\Delta t)$ and is first order (linear).

A.2 Backwards Euler Method

This technique can also be done backwards, implicitly, by solving for y_{n+1} rather than plugging in y_n. This is called the Backwards Euler Method and produces a difference equation from the derivative equation $\frac{dy}{dt} \approx \frac{(y_{n+1}-y_n)}{\Delta t} = f(t_{n+1}, y_{n+1})$ and is defined as

$$y_{n+1} = y_n + \Delta t f(t_{n+1}, y_{n+1}).$$

For example, consider the ODE $\frac{dy}{dx} = \alpha y$ with the initial condition $y(0) = y_0$. The Forward Euler Method produces the following

$$\begin{aligned}
y_1 &= y_0 + \Delta t(\alpha y_0) = y_0(1 + \alpha\Delta t) \\
y_2 &= y_1 + \Delta t(\alpha y_1) = y_0(1 + \alpha\Delta t) + \Delta t(\alpha y_0(1 + \alpha\Delta t)) = y_0(1 + \alpha\Delta t)^2 \\
&\vdots \\
y_n &= y_0(1 + \alpha\Delta t)^n.
\end{aligned}$$

The Backwards Euler Method produces

$$y_1 = y_0 + \Delta t(\alpha y_1) \Rightarrow y_1 - \Delta t(\alpha y_1) = y_0 \Rightarrow y_1 = y_0(1-\alpha\Delta t)^{-1}$$
$$y_2 = y_1 + \Delta t(\alpha y_2) \Rightarrow y_2 - \Delta t(\alpha y_2) = y_1 \Rightarrow y_2 = y_1(1-\alpha\Delta t)^{-2}$$
$$\vdots$$
$$y_n = y_0(1-\alpha\Delta t)^{-n}.$$

This method also has an error rate of $\mathcal{O}(\Delta t)$, but is harder to compute than the Forward Euler's Method because it may not be solvable directly. However, the Backwards Euler Method is better at reproducing the true behavior of a function that has an independent variable that grows or declines without bounds and has an asymptote for the dependent variable. This is because implicit methods are unconditionally stable where explicit methods are only conditionally stable. Take for example the ODE $\frac{dy}{dx} = -\alpha y, y(0) = y_0, \alpha > 0$, which has the exact solution $y(t) = y_0 e^{-\alpha t}$. Using the Forward Euler's Method, we have

$$y_1 = y_0 + \Delta t(-\alpha y_0) = y_0(1-\alpha\Delta t)$$
$$y_2 = y_1 + \Delta t(-\alpha y_1) = y_0(1-\alpha\Delta t) + \Delta t(\alpha y_0(1-\alpha\Delta t)) = y_0(1-\alpha\Delta t)^2$$
$$\vdots$$
$$y_n = y_0(1-\alpha\Delta t)^n.$$

Since the exact solution has a decaying exponent ($e^{-\alpha t}$) and approaches zero, then $y_n = y_0(1-\alpha\Delta t)^n$ only approaches zero if and only if $|1-\alpha\Delta t| < 1$. So if $\alpha\Delta t > 2$, then the function $y_n = y_0(1-\alpha\Delta t)^n$ approaches infinity and not zero. Therefore, it is only stable, and representative of the true nature of the solution, under the condition of $\alpha\Delta t < 2$. However, using the Backwards Euler Method, we have

$$y_1 = y_0 + \Delta t(-\alpha y_1) \Rightarrow y_1 - \Delta t(-\alpha y_1) = y_0 \Rightarrow y_1 = y_0(1+\alpha\Delta t)^{-1}$$
$$y_2 = y_1 + \Delta t(-\alpha y_2) \Rightarrow y_2 - \Delta t(-\alpha y_2) = y_1 \Rightarrow y_2 = y_1(1+\alpha\Delta t)^{-2}$$
$$\vdots$$
$$y_n = y_0(1+\alpha\Delta t)^{-n}.$$

This equation represents the decay of the exact equation much better than the previous method because $y_n = y_0(1+\alpha\Delta t)^{-n}$ approached zero for all $\Delta t > 0$ as long as $\alpha > 0$. Therefore, this method is unconditionally stable and the Forward Euler's Method is only conditionally stable.

A.3 Runge-Kutta Method

Computations may require a numerical method that has better accuracy. The Runge-Kutta (RK) method does a better job at approximations because it takes the slope values at four different points along the step and averages them. Overall, it has an error of $\mathcal{O}(\Delta t^5)$ per step and an accumulated $\mathcal{O}(\Delta t^4)$ error globally. Therefore, this is a fourth order method, where the Euler (forward and backwards) at first order methods. The RK method, using a fixed step size, can be calculated for a function $\frac{dy}{dt} = f(t,y)$ by

$$y_{n+1} = y_n + \frac{\Delta t}{6}[k_n^1 + 2k_n^2 + 2k_n^3 + k_n^4]$$

$$k_n^1 = f(t_n, y_n)$$

$$k_n^2 = f(t_n + \frac{\Delta t k_n^1}{2}, y_n + \frac{\Delta t}{2})$$

$$k_n^3 = f(t_n + \frac{\Delta t k_n^2}{2}, y_n + \frac{\Delta t}{2})$$

$$k_n^4 = f(t_n + \Delta t k_n^3, y_n + \Delta t).$$

This method requires more calculation per step than the Euler methods. However, with the Euler methods, there are actually more steps involved to get the same type of accuracy as the RK method. [2]

B Two-dimensional simplifications of the Hodgkin-Huxley Model

B.1 FitzHugh-Nagumo Model

By taking away the complexity of the Hodgkin-Huxley model, the FitzHugh-Nagumo model makes it possible to study topological properties of the system. Topological properties are the features in the system that remain qualitatively unaltered even with quantitative changes. There are four variables, the membrane potential $V(t)$ and three state variables $m(t)$, $n(t)$, and $h(t)$ in the Hodgkin-Huxley model. The FitzHugh-Nagumo model simplifies the system into just two variables.

Observe that in the Hodgkin-Huxley model, during an action potential both $V(t)$ and $m(t)$ have similar time scales and represent the excitability of the system. The sodium activation very nearly follows the dynamics of the membrane potential. Their similarities make it possible to combine $V(t)$ and $m(t)$ into a single activation variable, V. Likewise, $n(t)$ and $h(t)$ evolve on a time scale similar to each other but much slower than $V(t)$ and $m(t)$. Additionally, $h(t)$ is anti-correlated to $n(t)$ and can be rewritten as

$$h = 1 - n.$$

When $n(t)$ and $h(t)$ are plotted together, it is easy to see the nearly identical amplitude and time scale between the two variables. W represents the combination of $n(t)$ and $1 - n(t)$ and is characteristic of the refractoriness of the system. Figure 18 shows these relationships.

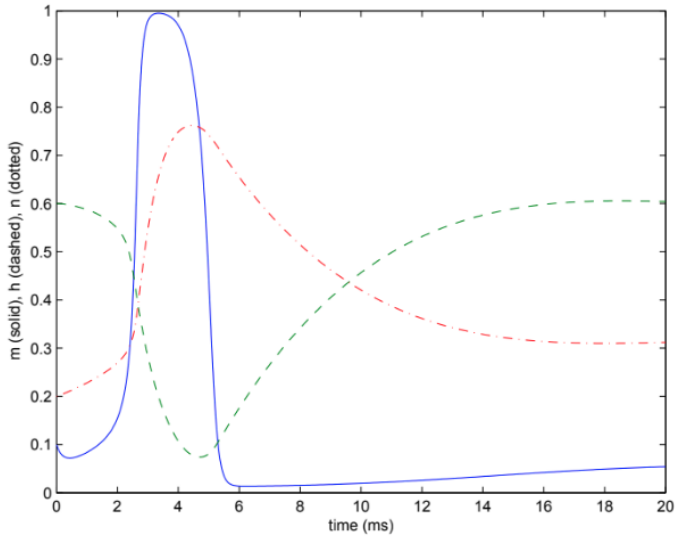

Figure 18: The solid blue curve shows the probablility of sodium activation m being permissive during an action potential. The green dashed curve shows the inactivation gate h and the red dashed-dotted curve is showing potassium activation.

When reduced in this way, the FitzHugh-Nagumo model is represented by

$$\frac{dV}{dt} = V - \frac{V^3}{3} - W + I$$
$$\frac{dW}{dt} = \phi(V + a - bW)$$

where a, b and ϕ are positive, dimensionless parameters that will be assumed to be 0.7, 0.8 and 0.08 respectively. The inverse of the time constant, represented by ϕ, makes it possible to control how fast W changes in relation to V. Notice how these equations are now in the form of a second-order autonomous system containing a single parameter much like the previous van der Pol example. Though, here the parameter is the injected current, I. Phase plane analysis on this system can be used to study its topological behavior without explicitly solving for solutions. First, finding the nullclines (when $V' = 0$ and $W' = 0$) will give an understanding of how the system evolves over time.

$$\frac{dV}{dt} = 0, \quad W = V - \frac{V^3}{3} + I$$
$$\frac{dW}{dt} = 0, \quad W = \frac{(V+a)}{b}$$

When the system is located on the V' nullcline, then it must move in a vertical direction from that point in the immediate future. If $W' > 0$ then the vertical motion is upwards, and downwards for $W' < 0$. Similarly, when located on the W' nullcline the system must move in a horizontal direction. Left when above the curve $W = V - \frac{V^3}{3} + I$ and right when below it.

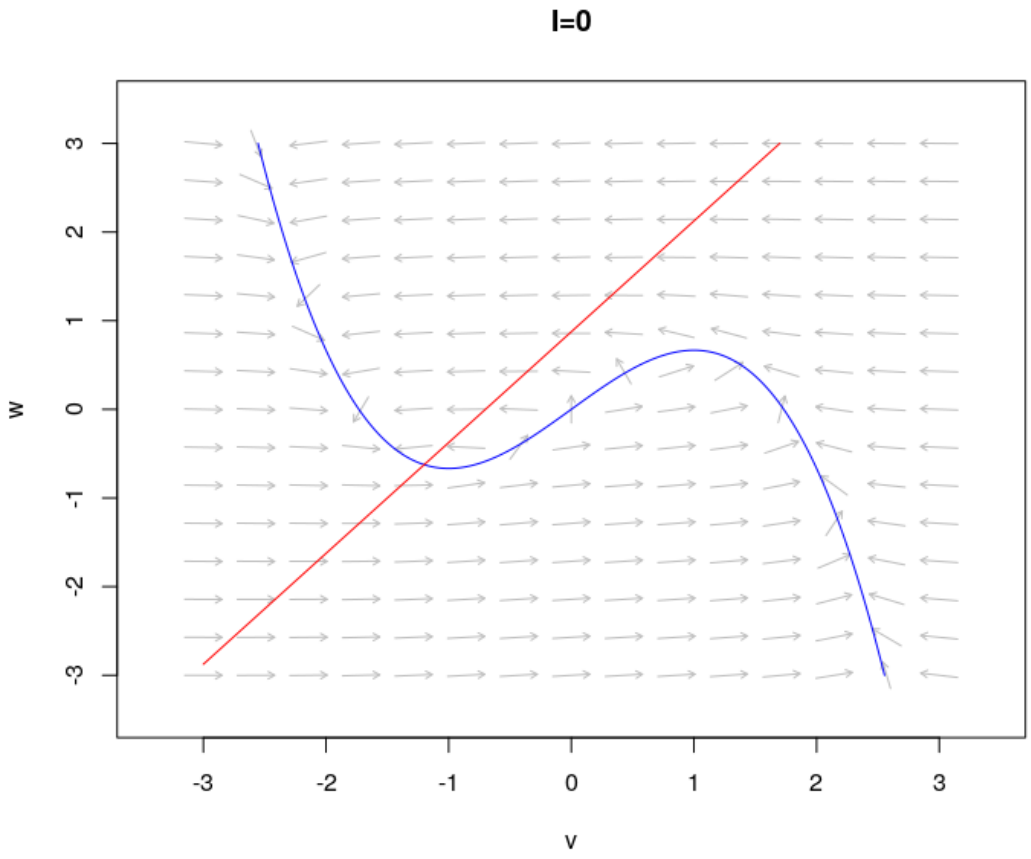

Figure 19: Nullclines of the FitzHugh-Nagumo model. The cubic curve (blue) is the V' nullcline and the line (red) represents W' nullcline. All directional arrows show the immediate future motion of the system when on the respective nullcline. Where the two curves intersect is the equilibrium solution to this model when $I = 0$, $a = 0.7$ and $b = 0.8$.

The two nullclines intersect at the point (-1.20, -0.624) when there is no applied current to the system ($I = 0$). Using the Jacobian matrix,

$$J = \begin{bmatrix} 1 - V^2 & -1 \\ \phi & -b\phi \end{bmatrix}, \quad tr(J) = (1 - V^2) + (-b\phi), \; and \; \det(J) = (1 - V^2)(-b\phi) - (\phi)(-1).$$

$$J = \begin{bmatrix} 1 - (-1.20)^2 & -1 \\ 0.08 & -0.064 \end{bmatrix} = \begin{bmatrix} -0.44 & -1 \\ 0.08 & -0.064 \end{bmatrix}$$

$$tr(J) = (-0.44) + (-0.064) = -0.504 \; and$$
$$\det(J) = (-0.44)(-0.064) - (0.08)(-1) = 0.108$$
$$tr(J)^2 - 4det(J) = -0.179$$

it is possible to determine that the equilibrium point is a spiral sink. When current is applied to the system it affects where the equilibrium point lies in the phase plane and has the potential to affect how

the system behaves. As the current is increased, the nullclines intersect at higher points along the W' nullcline. Breakdown of a stable equilibrium point occurs when the trace of the system changes from negative to positive. When there is applied current of $I = 0.33$ the two nullclines intersection moves to the point (-0.97, -0.34). Analyzing this new equilibrium using the Jacobian matrix,

$$J = \begin{bmatrix} 1-(-0.97)^2 & -1 \\ 0.08 & -0.06 \end{bmatrix} = \begin{bmatrix} 0.06 & -1 \\ 0.08 & -0.06 \end{bmatrix}$$

$$tr(J) = (0.06) + (-0.06) = 0 \; and$$

$$\det(J) = (0.06)(-0.06) - (0.08)(-1) = 0.076$$

$$tr(J)^2 - 4det(J) = -0.31$$

Looking at Figure 20, this change can be seen when the current changes from 0.32 to 0.33. The equilibrium point goes from being a spiral sink to being a spiral source and the entire system enters into a limit cycle. Thus, when $I = 0.33$ the system experiences a subcritical Hopf bifurcation, which is a feature of the Hodgkin-Huxley equations.

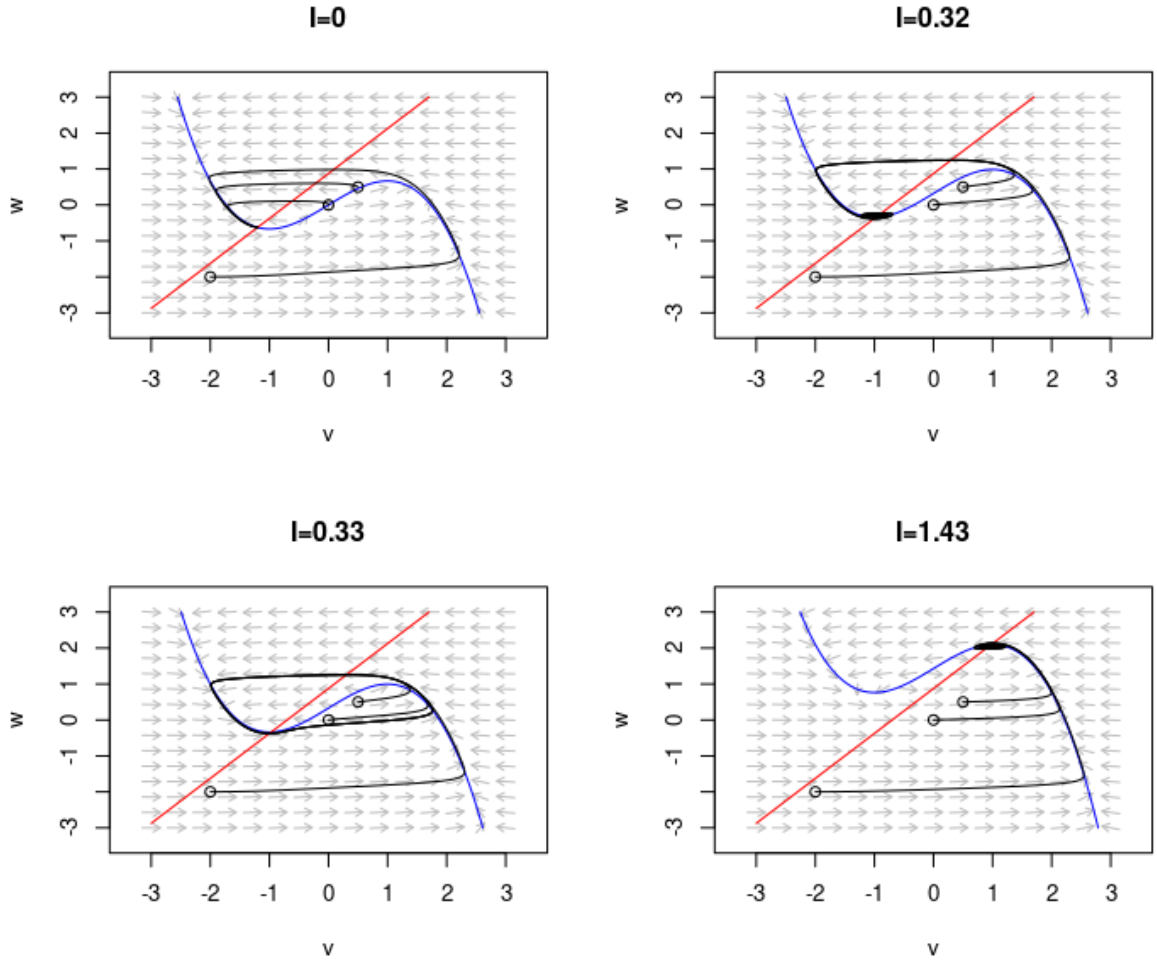

Figure 20: Phase plane portrait of the Fitz-Nagumo model with different applied currents (I_{ext}).

The strength of the FitzHugh-Nagumo model is in its ability to explain aspects of neuronal oscillations in response to an applied current. However, it is very simplistic and only captures one type of bifurcation found in the Hodgkin-Huxley model. The Morris-Lecar model can be used to demonstrate another way the onset of oscillation in a neuron can occur.

B.2 The Morris-Lecar Model

Though it was originally created to capture electrical impulses in the muscle fiber of a barnacle, the Morris-Lecar model can be used to model a different type of bifurcation seen in the Hodgkin-Huxley model. Additionally, this model qualitatively captures aspects of neural dynamics, such as various voltages and conductance's. The equations are

$$C_m \frac{dV_m}{dt} = -I_{ion}(V_m, w) + I_{ext}$$
$$\frac{dw}{dt} = \frac{w_\infty(V_m) - w}{\tau_w(V_m)}$$

where V_m is the membrane potential in mV, the membrane capacitance (C_m) is $1\mu F/cm^2$, w is the potassium activation in $\mu A/cm^2$ and t is time in ms. The only changing parameter of this model is the externally applied current (I_{ext}). The ionic current (I_{ion}) is the combination of calcium and potassium ionic current with the addition of a leaky gate,

$$I_{ion}(V_m, w) = \bar{g}_{Ca} m_\infty(V_m)(V_m - E_{Ca}) + \bar{g} w (V_m - E_K) + g_L(V_m - V_{rest})$$

such that $\bar{g}_{Ca} = 1.1$, $\bar{g}_K = 2.0$, $g_L = 0.5$, $E_{Ca} = 100$, $E_K = -70$, and $V_{rest} = -50$. Additionally, the change the calcium current happens much faster than the potassium current so the assumption is made that this is always at equilibrium where

$$m_\infty(V_m) = 0.5(1 + tanh\frac{V_m + 1}{15}).$$

The potassium ion current and the time constant are modeled by the the following equations respectively,

$$w_\infty(V_m) = 0.5(1 + tan\frac{V_m}{30}), \ and$$

$$\tau_w(V_m) = \frac{5}{cosh\frac{V_m}{60}}.$$

As with the FitzHugh-Nagumo model, this system can be analyzed without explicitly solving for solutions. Figure 21 shows the nullclines of V_m and w with no current applied ($I_{ext} = 0$) and with a current of $I_{ext} = 15$. Notice how the increase in current moves the equilibrium point along the curve $w' = 0$.

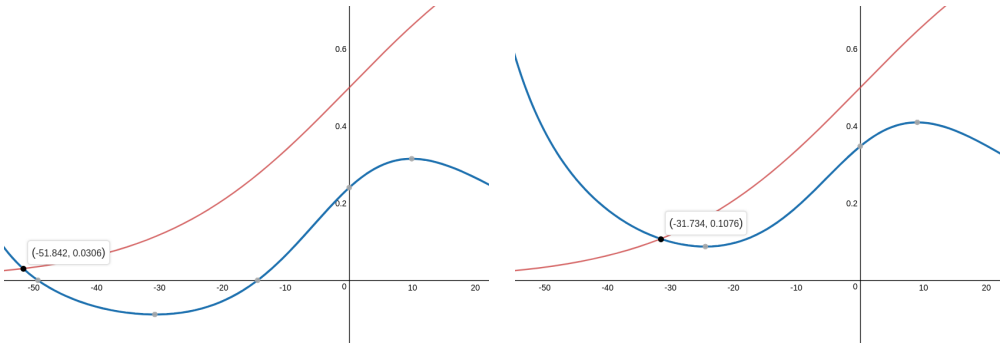

Figure 21: The nullclines of V_m and w. The left image is when no current applied ($I_{ext} = 0$) and the right is with a current of $I_{ext} = 15$.

When these two equilibrium points are studied using the same methods used with the FitzHugh-Nagumo equations it can be found that if the cell is depolarized to a resting potential of -31.7, then an applied current of 24.9 will send the system into a limit cycle. Any current below that will result in a stable equilibrium, see Figure 22. This type of behavior to a change in the parameter is similar to that seen in the FitzHugh-Nagumo model.

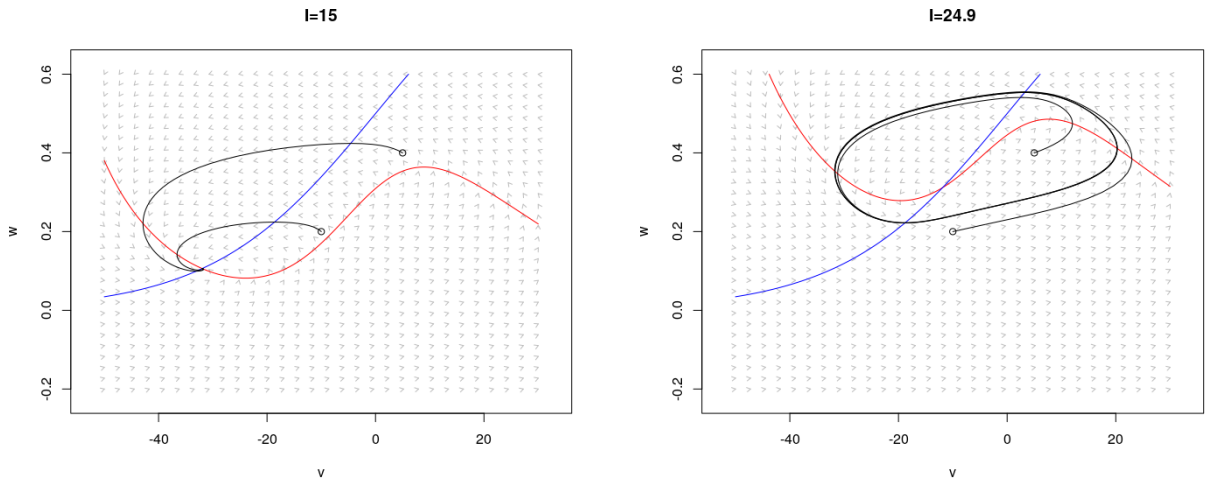

Figure 22: Hopf Bifurcation in the Morris-Lecar Model.

However, if this model is modified slightly it can reproduce a behavior seen in other types of cells that can generate oscillations with large intervals between spikes. Pyramidal cells found in the cortex can exhibit this type of behavior. In order to achieve this type of behavior from the Morris-Lecar equations, the nullclines must intersect more than once. To do this, the assumption that the potassium activation happens more abruptly than before. Thus, the following adjustments are made

$$w_\infty(V_m) = 0.5(1 + tan\frac{V_m - 10}{14.5}),$$

$$\tau_w(V_m) = \frac{3}{cosh\frac{V_m - 10}{29}}$$

and the conduction of calcium is reduced by 10% so that $\bar{g}_{Ca} = 1$. Now when the nullclines are evaluated when $I_{ext} = 0$, there are three equilibrium points.

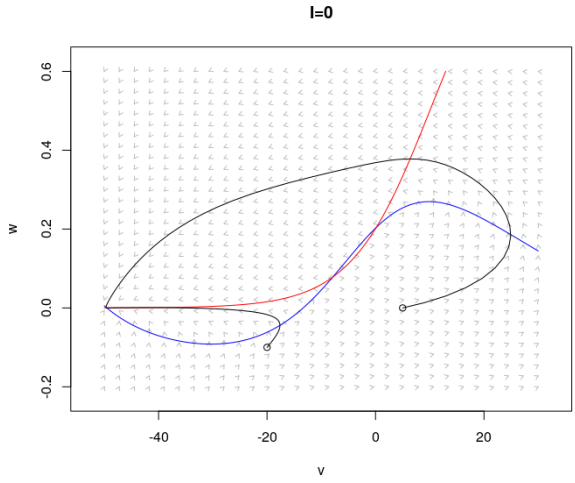

Figure 23: Modification of the Morris-Lecar model shows the occurrence of three equilibrium points.

The point to the left is a stable sink, the middle is unstable saddle and the right point is an unstable spiral. The presence of the unstable saddle introduces the idea of a threshold because the stable sink is globally attracting, thus the current input into the system may not always result in a spike. Any initial values of the system that start to the left of the unstable saddle point are directed to the stable sink. Any initial value that is to the right will cause a spike before settle back at the stable sink. Interestingly, if the initial values start close to the saddle point the system will move slowly before spiking or equalizing (Figure 23). Another quality of the modified Morris-Lecar equations is the occurrence of a saddle-node bifurcation. As the injected current is increased, the middle and upper right equilibrium points move closer together until they collide into a single equilibrium, which happens when the injected current reaches 8.326 (Figure 24).

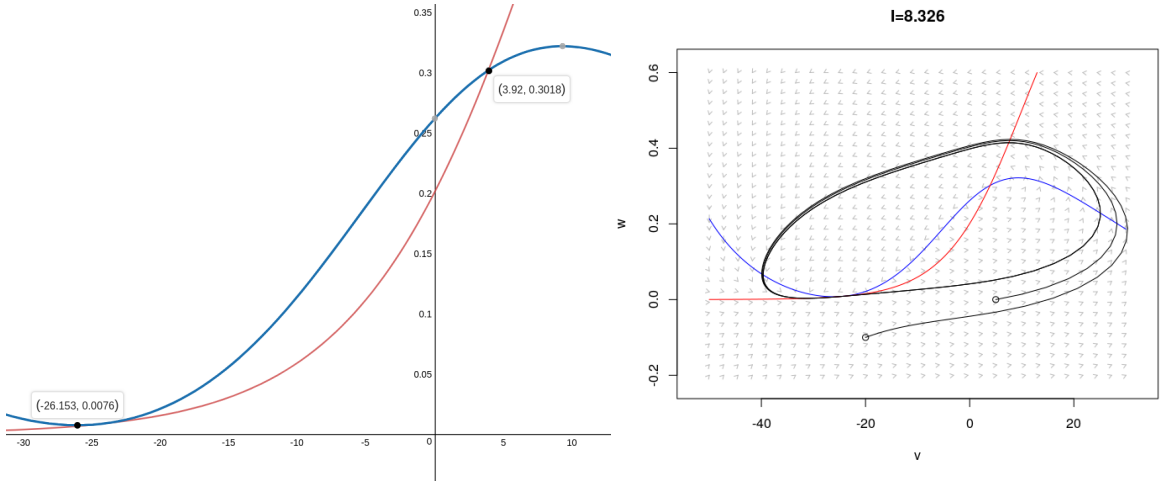

Figure 24: A saddle-node bifurcation of the Morris-Lecar model happens as the intersection of the lowest two equilibrium points occurs.

The areas around both of these equilibrium will take a long amount of time for the system to move to a different part of the system. Characteristic of the saddle-node bifurcations is an N-shaped curve. When V_m is plotted with time and the the current is set at or above 8.326, this shape can be easily identified (Figure 25). This shows the long pauses between spikes as well as the sharp increase in the potassium activation.

Both of these two-dimensional systems have their strengths and weaknesses. FitzHugh-Nagumo model is very simple and easy to use. It has the ability to enhance understanding of how a neurons complex system works on an elementary level. However, it is limited in its use and in its ability to explain more than two phenomenons found in neural dynamics. The Morris-Lecar model is still limited in its use but not nearly as much as the FitzHugh-Nagumo model but that also means the model is more complex and harder to use. Though, it has the ability to explain dynamics found in different types of neurons and matches more closely to the quantitative values seen in the Hodgkin-Huxley model. Both of these models, however, are useful in analyzing behaviors captured by Hodgkin and Huxley.

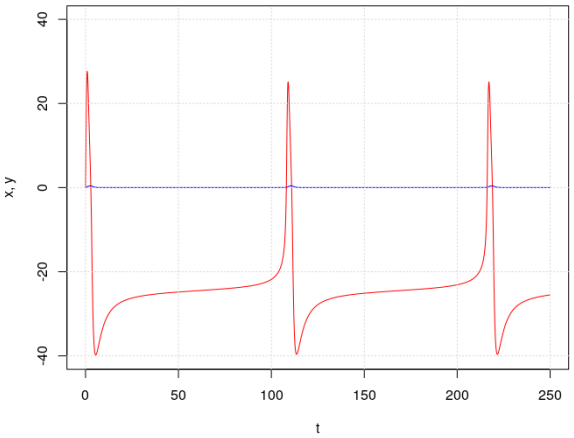

Figure 25: This N-shapped curve happens when the system takes a long time to get past the equilibrium points.

References

[1] The GIMP team. Gimp 2.8.10, 1997-2014.

[2] Eckhoff P et al. *A Short Course in Mathematical Neuroscience.* Princeton: Princeton UP, 2015.

[3] Terman D. Ermentrout GH. *Mathematical Foundations of Neuroscience.* Springer Science+Business Media, LLC, 2010.

[4] Historical impact: Discoveries with the squid giant axon led to the origins of modern neurobiology.

[5] E. Nelson, M. *Databasing the Brain: From Data to Knowledge.* Wiley, New York, 2004.

[6] Phase plane plotter : Built with processing and processing.js.

[7] Noonburg V. *Ordinary Differential Equations from Calculus to Dynamical Systems.* The Methematical Association of America, 2014.

[8] RStudio Team. *RStudio: Integrated Development Environment for R.* RStudio, Inc., Boston, MA, 2015.

[9] *Brain-computer interfaces : principles and practice.* Oxford University Press, Oxford: New York, 2012.

[10] C. Koch. *Biophysics of Computation.* Wiley, New York, 2004.

[11] P. Grindrod. *On Human Consciousness: A Mathematical Perspective.* University of Oxford, UK, 2017.

[12] T. Urban. *Neuralink and the Brain's Magical Future.* 2017.

[13] Burdge J. Overby J. *Chemistry: Atoms First.* McGraw-Hill Education, third edition, 2018.

[14] Khan Academy. Neuron action potentials: The creation of a brain signal, 2016.

Index